EXPERIMENTS AND COMPUTATIONAL MODELING OF PULVERIZED-CIAK IGNITION

Quarterly Technical Report

Reporting Period: 04/01/1997 through 06/30/1997

Author: John C. Chen

Report Issue Date: 08/01/1997

DE-FG22-96PC96221

North Carolina A&T State University
Department of Mechanical Engineering
1601 East Market Street
Greensboro, NC 27411

Disclaimer

Abstract

Under typical conditions of pulverized-coal combustion, which is characterized by fine particles heated at very high rates, there is currently a lack of certainty regarding the ignition mechanism of bituminous and lower rank coals. It is unclear whether ignition occurs first at the particle-oxygen interface (heterogeneous ignition) or if it occurs in the gas phase due to ignition of the devolatilization products (homogeneous ignition). Furthermore, there have been no previous studies aimed at determining the dependence of the ignition mechanism on variations in experimental conditions, such as particle size, oxygen concentration, and heating rate. Finally, there is a need to improve current mathematical models of ignition to realistically and accurately depict the particle-to-particle variations that exist within a coal sample. Such a model is needed to extract useful reaction parameters from ignition studies, and to interpret ignition data in a more meaningful way.

We propose to examine fundamental aspects of coal ignition through (1) experiments to determine the ignition mechanism of various coals by direct observation, and (2) modeling of the ignition process to derive rate constants and to provide a more insightful interpretation of data from ignition experiments.

We propose to use a novel laser-based ignition experiment to achieve our objectives. The heating source will be a pulsed, carbon-dioxide (CO_2) laser in which both the pulse energy and pulse duration are independently variable, allowing for a wide range of heating rates and particle temperatures — both of which are decoupled from each other and from the particle size. This level of control over the experimental conditions is truly novel in ignition and combustion experiments. Laser-ignition experiments also offer the distinct advantage of easy optical access to the particles because of the absence of a furnace or radiating walls, and thus permit direct observation and particle temperature measurement. The ignition mechanism of different coals under various experimental conditions can therefore be easily determined by direct observation with high-speed photography. The ignition rate-constants, when the ignition occurs heterogeneously, and the particle heating rates will both be determined from analyses based on direct, particle-temperature measurements using two-color pyrometry.

For the modeling portion of this study we will complete the development of the Distributed Activation Energy Model of Ignition (DAEMI), which simulates the conventional drop-tube furnace ignition experiment. The DAEMI accounts for particle-to-particle variations in reactivity

by having a single preexponential factor and a Gaussian distribution of activation energies among the particles. Previous results show that the model captures the key experimental observations, and that adjustments to the model parameters permit a good fit to experimental data. We will complete the model by (1) examining the effects of other variations in physical parameters on the model, (2) applying the model to published results in order to extract reaction parameters, and (3) extending the model for application to laser-based ignition studies, such as our own.

Table of Contents

Executive Summary

During the past reporting period, the design and construction of the two-wavelength pyrometer for particle-temperature measurement was completed. The photomultiplier tubes (PMTs) were placed inside housing units to shield them from light and to protect them from damage. The pyrometer was then integrated with the experiment, along with the data-acquisition system. The high-speed photography set-up has been designed and its construction is near completion. A commercial 35-mm camera will be used in conjunction with an optical chopper operated at high rotational a speed to acquire high-speed photographs of the ignition process.

We are continuing work on the manuscript to be submitted to *Energy and Fuels* for review.

Introduction

The ignition of pulverized coal has been the subject of research for nearly 150 years, with the initial motivation being the avoidance of coal-dust explosions in mines. In more recent times, due to the world's increased reliance on coal for power generation and the need to maximize energy-conversion efficiency, research has shifted to understanding the fundamental mechanism of coal ignition and measuring its kinetic rates. The importance of ignition to coal-flame stability is obvious — the more easily a particular coal ignites after injection into a boiler furnace, the better its flame-stability characteristics. A less obvious ramification of the ignition process is its role in establishing extended, fuel-rich zones in coal flames which are responsible for the destruction of NOx and its conversion to benign N_2. Certainly, the ignition process is inextricably linked to the formation of this NOx-reduction zone, and the ignition behavior of coals and coal blends will strongly affect the ease and extent of formation of this zone. This connection is deserving of further study and its understanding is the goal toward which we hope to apply the results of this proposed study. Specifically, we propose to examine fundamental aspects of coal ignition through (1) experiments to elucidate the ignition behavior of coals, and (2) modeling of the process to derive accurate and useful rate constants, and to provide a more insightful interpretation of data from ignition experiments.

Objectives

Our objectives for this project are to:

1. develop a novel experimental facility with extensive optical-diagnostic capabilities to study coal ignition;
2. determine the ignition mechanism of coals under simulated combustion conditions by direct observation with high-speed photography;
3. examine the effects of various experimental conditions, including coal rank, particle size, oxygen concentration and heating rate, on the ignition mechanism; and
4. measure the ignition rate constants of various coals.
5. modify our existing ignition model to examine the effect of particle-size distribution on the ignition behavior;

6. incorporate, if necessary, a size distribution into the model;
7. apply the model to extract ignition rate constants from previously published data from conventional experiments;
8. modify the model and apply it to our laser-based ignition studies for determination of ignition rate constants.

Results from This Reporting Period and Discussion

Experiment

During the last reporting period, we have designed and constructed the two-wavelength pyrometer for particle-temperature measurement. The system is shown schematically in Fig. 1. The pyrometer consists of photomutiplier tubes (PMT), which measure the intensity of the light from the ignition particles at two different wavelengths. A cylindrical housing shields each PMT from other sources of light and a fiber-optic scope directed at the experiment leads into each detector housing. Inside, the PMT is mounted onto a small base. The cylindrical housing is shown in Fig. 2. The optical scope enters through a hole in the front of the cylinder. The cylinder has a plate screwed to its top to block light entering from above. The plate is shown in Fig. 3.

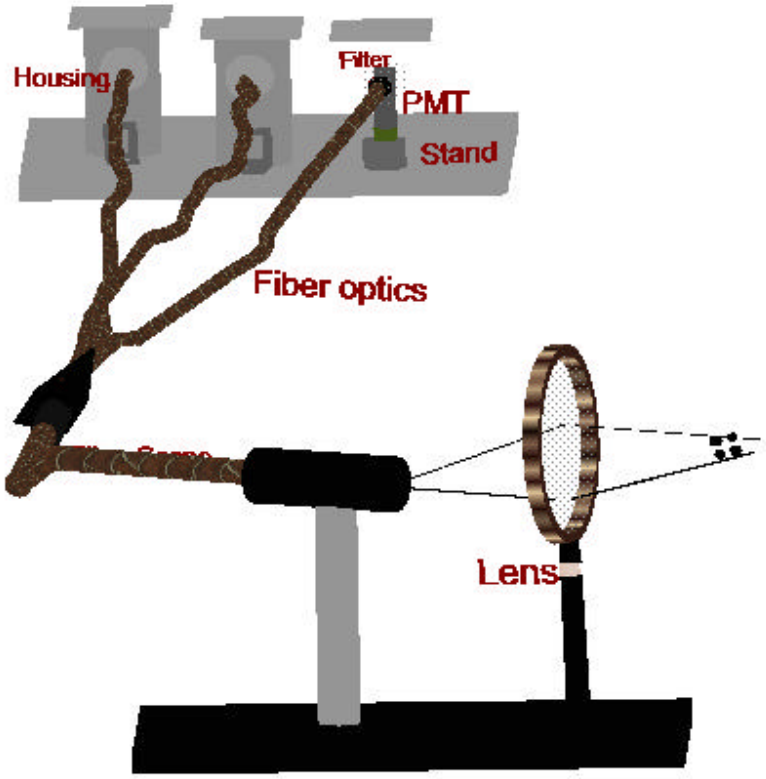

Fig. 1: Schematic showing the pyrometry system with three PMTs.

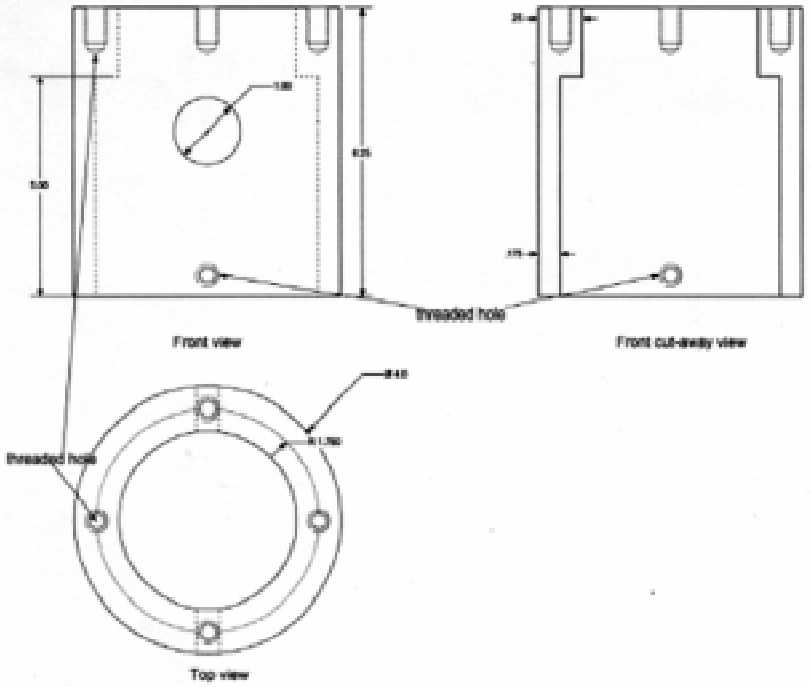

Fig. 2: Cylindrical housing for PMTs. Units are in inches.

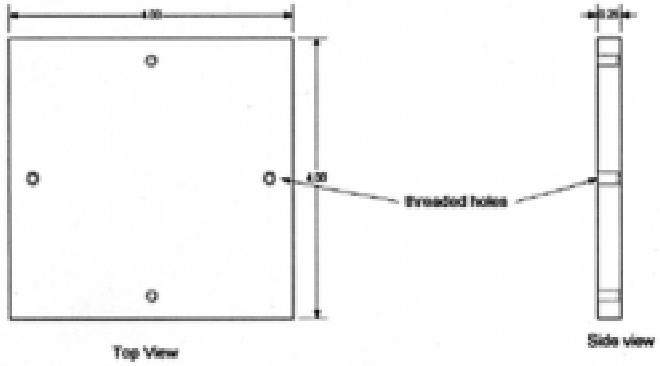

Fig. 3.: Top of housing. Units are in inches.

Another need of the design is to make sure that each individual PMT is held in place and does not move around in case the experiment is bumped. For this reason a pair of legs, shown in Fig. 4, are attached to the housing and a pair of clamps secure the legs to the optical table. The assembled PMT housing is shown in Fig. 5.

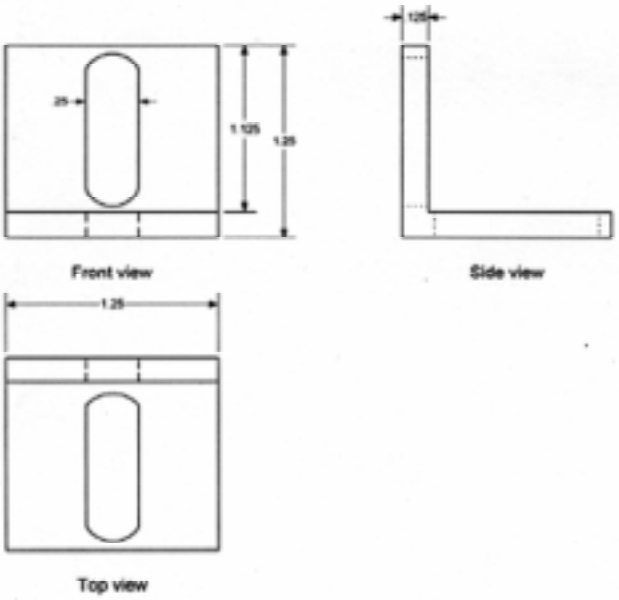

Fig. 4.: Legs for housing. Units are in inches.

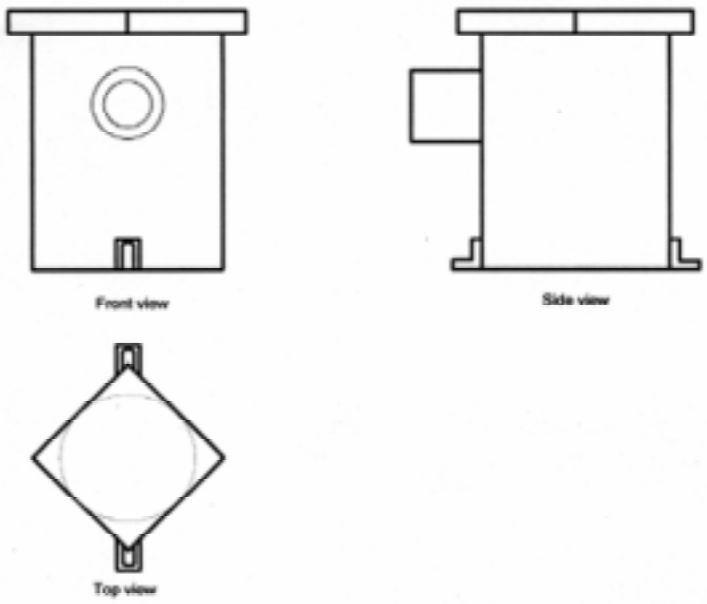

Fig. 5.: Assembled housing.

To stop the PMTs from moving around inside the housings a small base, shown in Fig. 6, is used to secure the PMTs. A pair of legs, shown in Fig. 7, are attached to the base and a pair of

clamps, Fig. 8, are used to secure these legs to the optical table. The component is shown with the PMT in Fig. 9.

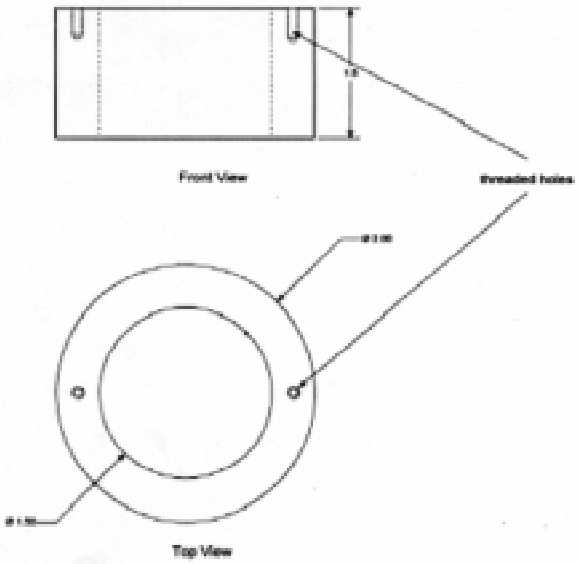

Fig. 6.: PMT Base. Units are in inches.

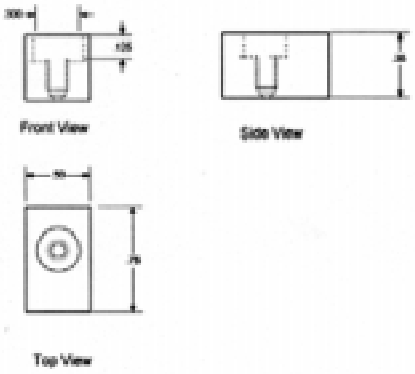

Fig. 7: Base legs. Units are in inches.

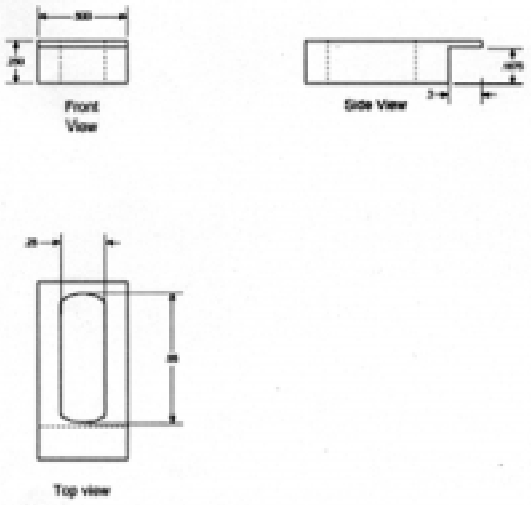

Fig. 8.: Base clamps. Units are in inches.

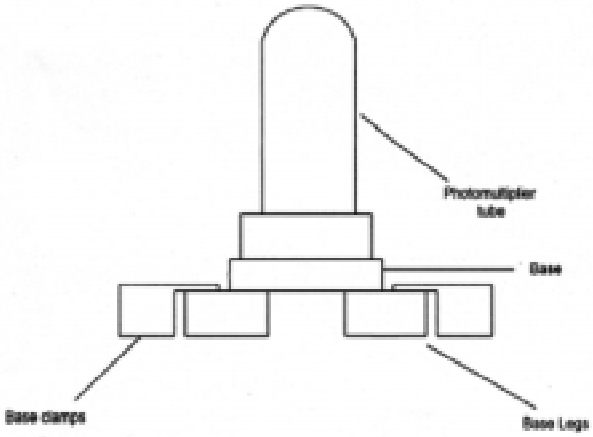

Fig. 9.: PMT in base setup.

Also during this reporting period the data-acquisition system has been set up for the purpose of recording signals from the PMTs. Data reduction will be conducted after each day's experiment using a personal computer.

The photography components have been received and a mounting has been prepared for the high-speed camera. A commercial 35-mm camera will be set up facing the experiment. In front of the camera will be an optical chopper operating at a high rotational speed to acquire high-speed

photographs of the ignition process. The photography setup is shown along with the experiment in Fig. 10.

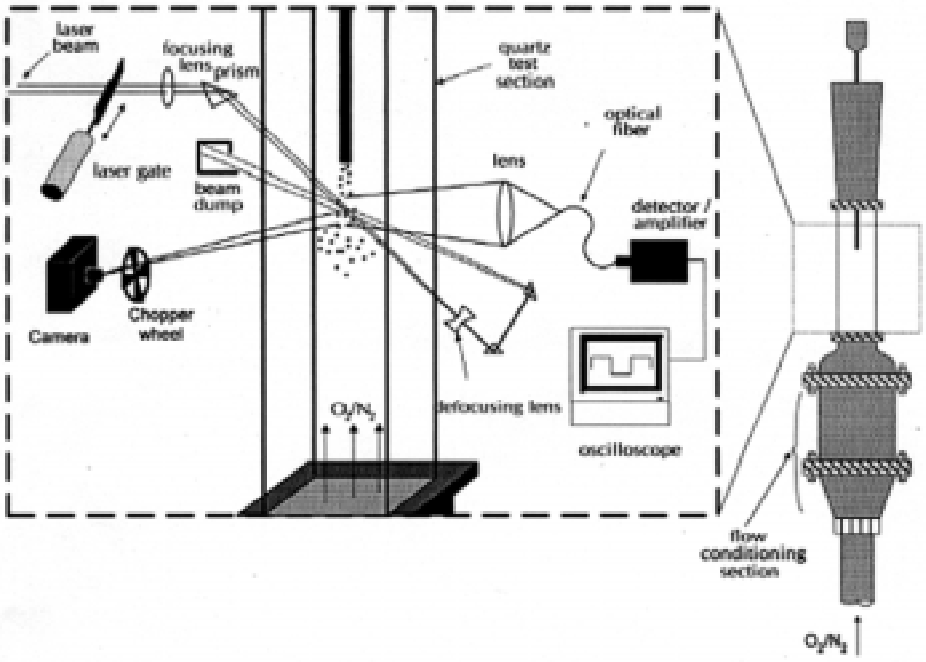

Fig.10: Experiment setup with high-speed photography system.

Goals for Next Quarter

During the next reporting period, we will test and refine the pyrometer and the high-speed photography system. After this is complete we will begin to run experiments to measure ignition temperatures of the particles under various conditions, and to extract ignition rate constants. The high-speed photographs will show the ignition mechanism of the coals, and provide insight into the combustion behavior.

EXPERIMENTS AND COMPUTATIONAL MODELING OF PULVERIZED COAL IGNITION

QUARTERLY TECHNICAL REPORT
07/01/97 TO 09/30/97

AUTHORS: JOHN C. CHEN

REPORT ISSUE DATE: 10/26/97

DE-FG22-96PC96221

NORTH CAROLINA A&T STATE UNIVERSITY
DEPARTMENT OF MECHANICAL ENGINEERING
1601 EASA MARKET STREET
GREENSBORO, NC 27411

Disclaimer

Abstract

Under typical conditions of pulverized-coal combustion, which is characterized by fine particles heated at very high rates, there is currently a lack of certainty regarding the ignition mechanism of bituminous and lower rank coals. It is unclear whether ignition occurs first at the particle-oxygen interface (heterogeneous ignition) or if it occurs in the gas phase due to ignition of the devolatilization products (homogeneous ignition). Furthermore, there have been no previous studies aimed at determining the dependence of the ignition mechanism on variations in experimental conditions, such as particle size, oxygen concentration, and heating rate. Finally, there is a need to improve current mathematical models of ignition to realistically and accurately depict the particle-to-particle variations that exist within a coal sample. Such a model is needed to extract useful reaction parameters from ignition studies, and to interpret ignition data in a more meaningful way.

We propose to examine fundamental aspects of coal ignition through (1) experiments to determine the ignition mechanism of various coals by direct observation, and (2) modeling of the ignition process to derive rate constants and to provide a more insightful interpretation of data from ignition experiments.

We propose to use a novel laser-based ignition experiment to achieve our objectives. The heating source will be a pulsed, carbon-dioxide (CO_2) laser in which both the pulse energy and pulse duration are independently variable, allowing for a wide range of heating rates and particle temperatures — both of which are decoupled from each other and from the particle size. This level of control over the experimental conditions is truly novel in ignition and combustion experiments. Laser-ignition experiments also offer the distinct advantage of easy optical access to the particles because of the absence of a furnace or radiating walls, and thus permit direct observation and particle temperature measurement. The ignition mechanism of different coals under various experimental conditions can therefore be easily determined by direct observation with high-speed photography. The ignition rate-constants, when the ignition occurs heterogeneously, and the particle heating rates will both be determined from analyses based on direct, particle-temperature measurements using two-color pyrometry.

For the modeling portion of this study we will complete the development of the Distributed Activation Energy Model of Ignition (DAEMI), which simulates the conventional drop-tube furnace ignition experiment. The DAEMI accounts for particle-to-particle variations in reactivity

by having a single preexponential factor and a Gaussian distribution of activation energies among the particles. Previous results show that the model captures the key experimental observations, and that adjustments to the model parameters permit a good fit to experimental data. We will complete the model by (1) examining the effects of other variations in physical parameters on the model, (2) applying the model to published results in order to extract reaction parameters, and (3) extending the model for application to laser-based ignition studies, such as our own.

Table of Contents

Executive Summary

During the past reporting period, we have completed an analysis to optimize our two-color pyrometry system and examine its performance characteristics. We have begun the first set of experiments to test the pyrometry system, as well as the high-speed photography system.

Introduction

The ignition of pulverized coal has been the subject of research for nearly 150 years, with the initial motivation being the avoidance of coal-dust explosions in mines. In more recent times, due to the world's increased reliance on coal for power generation and the need to maximize energy-conversion efficiency, research has shifted to understanding the fundamental mechanism of coal ignition and measuring its kinetic rates. The importance of ignition to coal-flame stability is obvious — the more easily a particular coal ignites after injection into a boiler furnace, the better its flame-

stability characteristics. A less obvious ramification of the ignition process is its role in establishing extended, fuel-rich zones in coal flames which are responsible for the destruction of NOx and its conversion to benign N_2. Certainly, the ignition process is inextricably linked to the formation of this NOx-reduction zone, and the ignition behavior of coals and coal blends will strongly affect the ease and extent of formation of this zone. This connection is deserving of further study and its understanding is the goal toward which we hope to apply the results of this proposed study. Specifically, we propose to examine fundamental aspects of coal ignition through (1) experiments to elucidate the ignition behavior of coals, and (2) modeling of the process to derive accurate and useful rate constants, and to provide a more insightful interpretation of data from ignition experiments.

Objectives

Our objectives for this project are to:

1. develop a novel experimental facility with extensive optical-diagnostic capabilities to study coal ignition;
2. determine the ignition mechanism of coals under simulated combustion conditions by direct observation with high-speed photography;
3. examine the effects of various experimental conditions, including coal rank, particle size, oxygen concentration and heating rate, on the ignition mechanism; and
4. measure the ignition rate constants of various coals.
5. modify our existing ignition model to examine the effect of particle-size distribution on the ignition behavior;
6. incorporate, if necessary, a size distribution into the model;
7. apply the model to extract ignition rate constants from previously published data from conventional experiments;
8. modify the model and apply it to our laser-based ignition studies for determination of ignition rate constants.

Results from This Reporting Period and Discussion

Personnel

We have recruited a student, Ms. Jianping Zheng, for work on this project related to the computational model development. Ms. Zheng is a new student in the department's MS program.

Computational Model

During the past reporting period, we have begun the modification of the Distributed Activation Energy Model of Ignition (DAEMI) to model our laser-ignition experiment. We are examining the effects of varying numbers of particles which are intercepted by the laser pulse on the model's predictions, as well as the effect of a distribution of particle size in addition to a distribution of activation energy. We expect to complete the modifications and report on the results in the next reporting period.

Experiment

Two reporting periods ago, we reported on the design and construction of our two-color pyrometry system. During the past reporting period, we optimized the pyrometry system's components, and examined the expected performance. These findings are summarized below.

1. Theory of Operation

This section describes the operational principles and expected performance of a two-wavelength pyrometer used for particle-temperature measurement. The specific application in this instance is the measurement of pulverized coal temperatures *at ignition* in an experiment where one to five particles are ignited by a high-energy laser pulse. The light emitted by the igniting particles is collected by a train of optics, divided into two or three light paths via a trifurcated optical-fiber bundle, passed through a narrow bandpass interference filter, and finally detected by a photomultiplier tube (PMT). Here we will examine the expected signal levels at the pyrometer, and gauge the instrument's temperature-measurement sensitivity.

We will assume coal particles to be gray, and thus emit light according to Planck's blackbody spectral distribution, modified by its coefficient of emissivity:

$$E_\lambda(T) = \frac{\varepsilon C_1}{\lambda^5\left[\exp\left(\frac{C_2}{\lambda T}\right) - 1\right]}, \qquad (1)$$

where ε is the coal emissivity, λ is the wavelength, and T is the particle temperature. C_1 and C_2 are the usual constants for Planck's spectral distribution.

A very good approximation (<1% error at all wavelengths) to Planck's distribution is:

$$E_\lambda(T) \approx \frac{\varepsilon C_1}{\lambda^5} \exp\left(\frac{-C_2}{\lambda T}\right), \tag{2}$$

and we will make use of this approximation for the remainder of this paper. The units of Eq. (1) or (2) are $\left[\frac{W}{m^2 \cdot \mu m}\right]$, since each describes the power emitted by a gray body, per surface area, within an infinitesimally small wavelength interval.

A two-wavelength, or two-color, pyrometer works on the principle that the temperature of a gray surface or a blackbody can be determined simply by measuring the light (power) emitted by that surface at two *separate but known* wavelengths. This principle is easily verified by examining Eq. (2), in which the variable, E_λ (which is measured in the experiment), is dependent on λ and on T. Thus, if E_{λ_1} and E_{λ_2}, which represent the power measured at wavelengths λ_1 and λ_2, respectively, were measured, the ratio of the powers, $E_{\lambda_1}/E_{\lambda_2}$, would yield the single unknown, T:

$$\frac{E_{\lambda 1}}{E_{\lambda 2}} = \left(\frac{\lambda_2}{\lambda_1}\right)^5 \exp\left[\frac{-C_2}{T}\left(\frac{1}{\lambda_1} - \frac{1}{\lambda_2}\right)\right]. \tag{3}$$

The importance of the assumption of blackbody or gray body (constant ε) is now obvious from examining Eq. (3), where the ratio of emissivities at the two wavelengths is assumed to be unity. The actual determination of the power emitted by the particles is complicated by the fact that various optical components lie in the path between the particle and the detector, and that the detector has variable response, depending on the wavelength of light falling on it. Nevertheless, the general principle of operation of the two-color pyrometer is as described above.

We now develop a more rigorous expression of the power detected at the PMT, in order to determine the expected pyrometer performance. The *intensity* of light given off by a gray body at temperature T is:

$$I_\lambda(T) = \frac{\varepsilon C_1}{\pi \lambda^5} \exp\left(\frac{-C_2}{\lambda T}\right) [=] \frac{W}{m^2 \cdot \mu m \cdot sr} . \quad (4)$$

Note that the principal difference between Eq. (2) and (4) is that the latter is the power emitted by a gray body, per unit surface area, per infinitesimally small wavelength interval, and per infinitesimally small solid angle. These dependencies are shown schematically below.

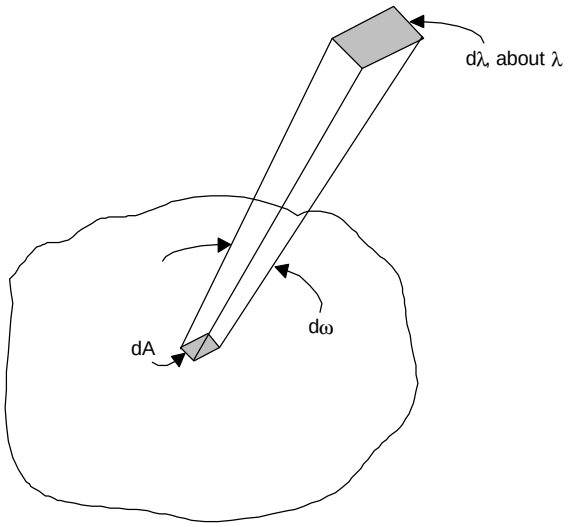

Figure 1: Schematic showing nomenclature for Planck's spectral power distribution.

The typical experimental set-up currently in use in our lab is shown in the figure below, assuming that only a single particle is in view (if multiple particles are present, the analysis remains the same, except for the inclusion of a multiplication factor equal to the number of particles).

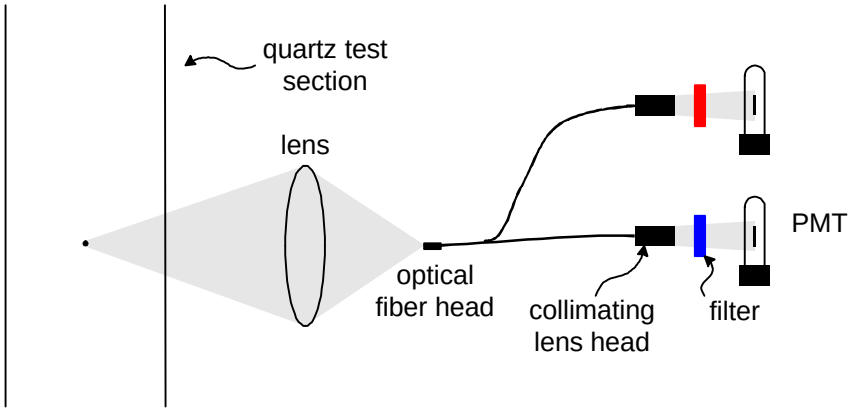

Figure 2: Layout of pyrometer set-up used for particle temperature measurement. Note that a third detection channel may be included, if desired.

Loss of light from the igniting particle occurs as the light passes through each optical component due to reflections, and the power that finally arrives at the detection surface of each PMT is given by:

$$P = \left[\frac{\varepsilon C_1}{\pi\lambda^5}\exp\left(\frac{-C_2}{\lambda T}\right)\right][A\Omega][\Delta\lambda]\tau_{\substack{\text{test}\\\text{sec tion}}}\tau_{\text{lens}}\tau_{\substack{\text{optical}\\\text{fiber}}}\tau_{\substack{\text{lens}\\\text{head}}}\tau_{\text{filter}}\tau_{\substack{\text{PMT}\\\text{window}}} \quad (5)$$
$$= I_\lambda(T)\cdot A\Omega\cdot\Delta\lambda\cdot\tau_{\text{loss}}[=]\ \text{W}.$$

In words, the power that arrives at the PMT detection surface is simply the gray body's emitted intensity (I_λ), times the area-solid angle factor ($A\Omega$, or etendue), times the spectral bandwidth of the filter ($\Delta\lambda$), and finally multiplied by a factor which accounts for all the transmission losses of the optical components in the system. In the expression for P, I_λ depends on the particle temperature (which is what we seek) and the wavelength of the chosen filter, $\Delta\lambda$ depends on the bandwidth (FWHM) of the filter, and both the etendue and τ_{loss} depend on the optical system. Note, however, that the both these factors (etendue and τ_{loss}) are fixed, and does not change from run to run, so long as the optical system does not change. While Eq. (5) can be used to calculate the power detected by the PMT, and can even be used to determine the particle temperature in a single-color pyrometer, the solution is highly uncertain due mainly to the uncertainties in the particle emissivity, the etendue, and the various transmission losses. This uncertainty is the reason that two-color pyrometers are more favored.

To complete this analysis, the signal (S), as an electrical current, developed by the PMT is simply:

$$S = I_\lambda(T)\cdot A\Omega\cdot\Delta\lambda\cdot\tau_{\text{loss}}\cdot R_\lambda \quad (6)$$

where S has units of amps. R_λ is referred to as the PMT's *responsivity*, and has units of A/W. (The subscript on responsivity is a reminder that this value is a function of the wavelength of light that

strikes it.) Input of this current into an appropriate current-to-voltage converter will then produce a voltage for detection.

Starting with Eq. (6), it is now possible to develop an expression for the ratio of two signals from a two-color pyrometer:

$$\frac{S_1}{S_2} = \left(\frac{I_{\lambda 1}}{I_{\lambda 2}}\right)\left(\frac{\Delta\lambda_1}{\Delta\lambda_2}\right)\left(\frac{\tau_{loss,1}}{\tau_{loss,2}}\right)\left(\frac{R_{\lambda 1}}{R_{\lambda 2}}\right), \tag{7}$$

where the subscripts 1 and 2 refer to the two colors or signal paths in the pyrometer. In Eq. (7), notice that while the etendue for each signal path divides out, the transmission loss does not, since the loss due to optical components are in general dependent on the wavelength of light (e.g. transmission loss in the optical fiber is higher for shorter wavelengths than for long wavelengths). Substituting for the gray body intensity Eq. (4) and rearranging, Eq. (7) becomes:

$$\begin{aligned}\frac{S_1}{S_2} &= \left[\frac{I_{\lambda 1}}{I_{\lambda 2}}\right]\left(\frac{\Delta\lambda_1}{\Delta\lambda_2}\right)\left(\frac{\tau_{loss,1}}{\tau_{loss,2}}\right)\left(\frac{R_{\lambda 1}}{R_{\lambda 2}}\right) \\ &= \left[\left(\frac{\varepsilon_1}{\varepsilon_2}\right)\left(\frac{\lambda_2}{\lambda_1}\right)^5 \exp\left(\frac{-C_2}{T}\left(\frac{1}{\lambda_1}-\frac{1}{\lambda_2}\right)\right)\right]\left(\frac{\Delta\lambda_1}{\Delta\lambda_2}\right)\left(\frac{\tau_{loss,1}}{\tau_{loss,2}}\right)\left(\frac{R_{\lambda 1}}{R_{\lambda 2}}\right)\end{aligned} \tag{8}$$

Assuming that coal behaves as a gray body (ε does not depend on wavelength), the ratio of emissivities becomes one, and Eq. (8) can be regrouped to become:

$$\frac{S_1}{S_2} = \left(\frac{\lambda_2}{\lambda_1}\right)^5 \exp\left(\frac{-C_2}{T}\left(\frac{1}{\lambda_1}-\frac{1}{\lambda_2}\right)\right)K, \tag{9}$$

where the calibration constant, K, is defined as:

$$K \equiv \left(\frac{\Delta\lambda_1}{\Delta\lambda_2}\right)\left(\frac{\tau_{loss,1}}{\tau_{loss,2}}\right)\left(\frac{R_{\lambda 1}}{R_{\lambda 2}}\right). \tag{10}$$

K is determined using Eq. (9) by directing the pyrometer at a blackbody source whose temperature is accurately known and by measuring the signals at the two wavelengths. The measured signals are then plugged into the rearranged Eq. (9):

$$K = \left(\frac{S_1}{S_2}\right)\left(\frac{\lambda_1}{\lambda_2}\right)^5 \exp\left[\frac{C_2}{T}\left(\frac{1}{\lambda_1} - \frac{1}{\lambda_2}\right)\right]. \quad (11)$$

This calibration eliminates the need to know accurately the transmission losses, filter bandwidths, and PMT responsivities, and is the main reason that two-color pyrometers are more often used than single-color pyrometers.

Once K is determined from calibration, the pyrometer is ready for use to measure particle temperatures. Directing the pyrometer now at igniting coal particles and measuring the signals, S_1 and S_2, these values are plugged into the following equation, which is simply a rearrangement of Eq. (9), in order to determine the particle temperature:

$$T = \frac{-C_2\left(\frac{1}{\lambda_1} - \frac{1}{\lambda_2}\right)}{\ln\left[\frac{1}{K}\left(\frac{S_1}{S_2}\right)\left(\frac{\lambda_1}{\lambda_2}\right)^5\right]}. \quad (12)$$

To get an idea of a two-color pyrometer's sensitivity for measuring temperatures, we can plot S_1/S_2 from Eq. (8) versus T for various pairs of filter (each with a different center wavelength and optical bandwidth), and assuming some reasonable values for the transmission losses. The responsivities used are typical wavelength-dependent values supplied by the PMT vendor. The following cases are considered:

	Filter 1		Filter 2	
	Center wavelength λ, nm	Filter bandwidth $\Delta\lambda$, μm	Center wavelength λ, nm	Filter bandwidth $\Delta\lambda$, μm
Case 1	400	10	800	10
Case 2	400	40	800	10
Case 3	600	10	700	10
Case 4	500	10	600	10
Case 5	500	40	600	10
Case 6	500	40	700	10

The results of these calculations are shown in Figure 3, where the ratio, S_1/S_2, is plotted as a function of particle temperature. The K values shown are calculated using Eq. (10) above, assuming

$\tau_{loss,1}$=0.75 and $\tau_{loss,2}$=0.5, and the responsivities, $R_{\lambda 1}$ and $R_{\lambda 2}$, are taken from the data sheet provided by the PMT manufacturer. These calculations are for illustrative purposes only, so the exactness of the values used is unimportant.

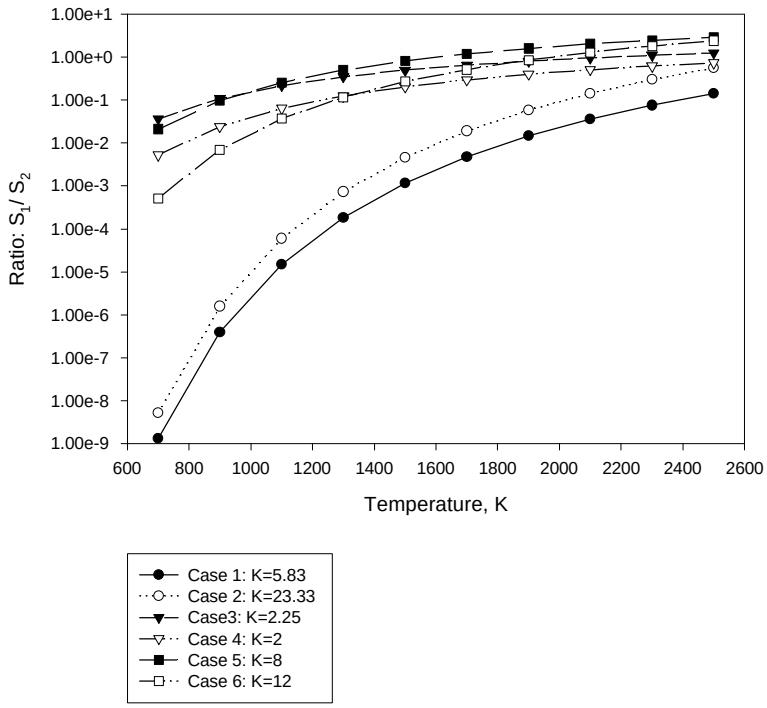

Figure 3: Plot of calculated signal ratios, S_1/S_2, versus temperature of body being observed by pyrometer. Case number is referenced to table above, and values of K are calculated using Eq. (10).

It can be seen in Figure 3 that the highest sensitivity to temperature, or the largest slope, $\frac{d\left(\frac{S_1}{S_2}\right)}{dT}$, occurs for cases 1 and 2, while the lowest pyrometer sensitivity in pyrometer performance occurs in cases 3, 4 and 5. It can be concluded from these calculations that the best pyrometer performance occurs when λ_1 and λ_2 are widely separated in wavelength, while the bandwidth of the filters is of secondary importance (as shown by the comparable sensitivity of cases 4 and 5). There is, however, one further consideration: At very short wavelengths, the signal may be so low (due to the nature of Planck's blackbody distribution function and the low PMT responsivity) that it is at a level near or below the noise level. Thus, while the goal should be to maximize the separation of the two wavelengths of the filters chosen for the pyrometer, the lower wavelength is also limited by the detection limit set by the signal-to-noise ratio. These observations can be confirmed by taking the derivative of S_1/S_2 (Eq. (9)) with respect to T.

2. System Design

The layout of the system is shown in Figure 4. The receiving optics (lens and optical fiber bundle) of the pyrometer is shown to the right of the test section, and the calibration source is to the left. The path of the calibration beam is shaded in gray while the path of the light captured by the receiving optics is outlined only. The outline is present on the region between the center of the test section and the achromat lens to denote that the two lenses have been matched to capture the same solid angle. This point will be explained in detail later. The high-speed camera system is shown in its position, viewing the ignition point at an angle through a chopper wheel.

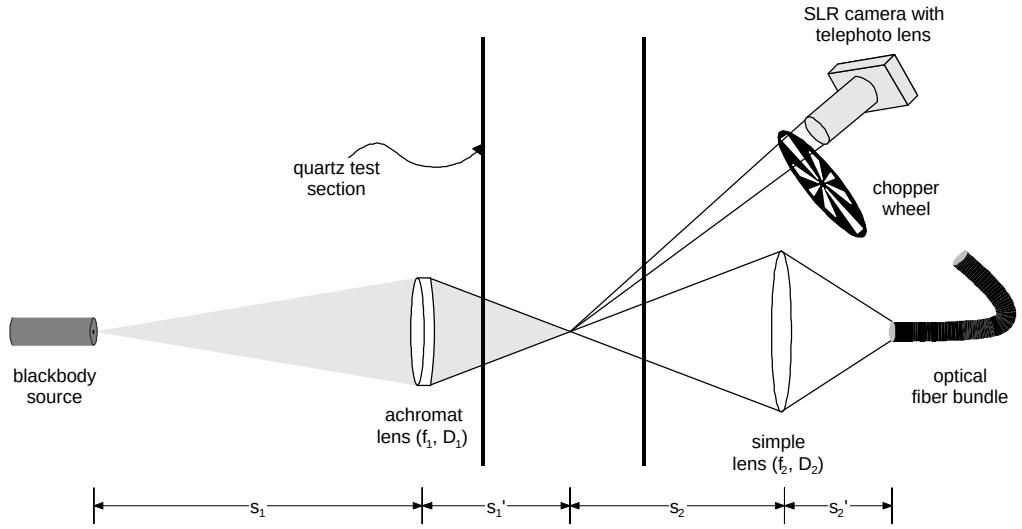

Figure 4: Schematic showing layout of pyrometry system relative to experiment, including receiving optics, calibration (blackbody) source, and high-speed photography system.

The starting point for the design of the optical system is the constraint that we will be dealing with extremely low light levels – as low as the light emitted by a single 100-μm coal particle at 500°C. Thus, the need to maximize the amount of light that is collected by the receiving, or detection, optics, drives our system design. The fiber-optic bundle can receive light input at a maximum total angle of 68°; no standard lens is this fast. Our system therefore will be limited by the "speed" of the simple lens, and we simply choose the "fastest" (lowest f/D, or focal length-to-diameter ratio) lens we can find. For our system, we've chosen an f=62.9 mm/D=50.8 mm lens, giving a f/D of 1.23.

To determine the location of the receiving lens, we consider that the diameter of the fiber-optic bundle is 5.5 mm, which is approximately one-half the diameter of the area from which we

want to detect igniting particles. We make this choice even though the actual ignition point is only ~2-3 mm in diameter in order to give a margin of error for alignment and for particle motion. This choice of detection area means that we want 2:1 imaging, or a magnification of 0.5. With this constraint we can now calculate the distances s_2 and s_2' shown in Figure 4. The lens equation is:

$$\frac{1}{s_2} + \frac{1}{s_2'} = \frac{1}{f_2}, \tag{13}$$

which relates the object distance (s_2), the image distance (s_2'), and the focal length of the lens. The additional constraint is the magnification (M) of 0.5:

$$M = \frac{s_2'}{s_2} = 0.5. \tag{14}$$

Substituting Eq. (14) into Eq. (13), we find that for 2:1 imaging:

$$s_2 = 2s_2', \text{ and}$$

$$2s_2' = 3f,$$

and using f_2=62.9 mm in this case gives s_2'=94.4 mm (3.7 in.) and s_2=188.7 mm (7.4 in.).

We now move to the specification of the optics for the calibration source. Here we have two considerations: (1) the need to match the solid angle subtended by the receiving optics to the image of the calibration source, as shown in Figure 4 (that is, we want to fill the receiving lens with the light from the calibration source, just as igniting particles would); and (2) the desired demagnification of the calibration source, which is a 1-mm diameter blackbody source.

To satisfy the first consideration, we want to match the angles, α_1 and α_2, shown in Figure 5. The two lenses have different diameters, and to match the angles, we simply note the similar angles:

$$\alpha_1 = \alpha_2$$

$$\frac{s_1'}{D_1} = \frac{s_2}{D_2}$$

s_2 and D_2 are set from our previous consideration, and we choose D_1 to be 25 mm, since a fast achromat lens is much more widely available in this size than in the 50 mm version. (The need for an achromat lens is explained later.) This choice results in s_1'=92.9 mm (3.7 in.).

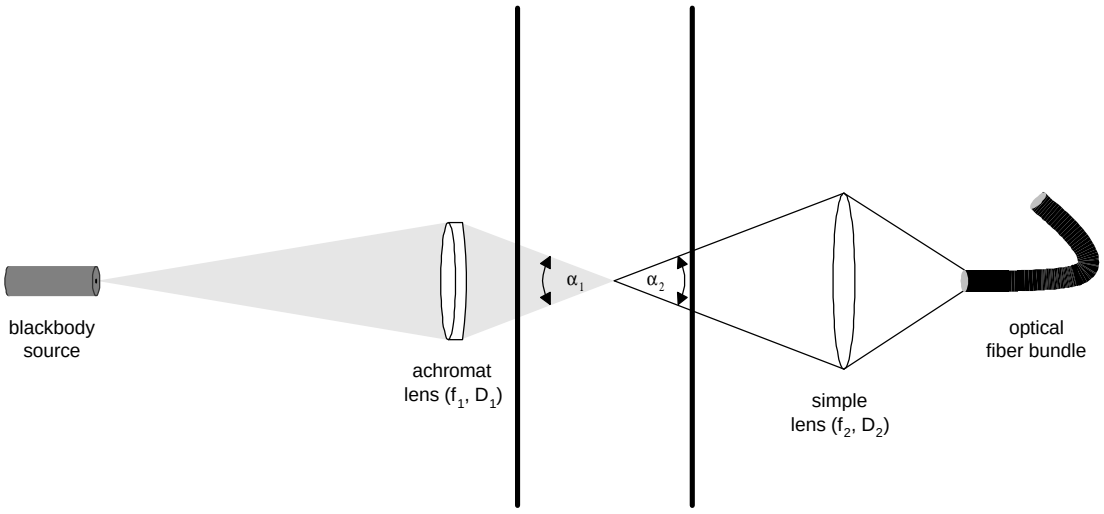

Figure 5: Schematic showing the angles subtended by the calibration-source imaging optics, and the receiving optics.

The second consideration involves the chosen demagnification of the calibration source. The coals we will use are in the size range of 60-200 μm diameter, and the blackbody source is 1 mm in diameter. Thus, a demagnification factor of 3 to 10 (M=1/3 to 1/10) is desired to simulate the possible range of particle size and numbers we might encounter in the experiment. To specify the lenses' focal length and s_1, we again apply the lens equation and the definition of magnification:

$$M = \frac{s_1'}{s_1}$$

$$\frac{1}{s_1} + \frac{1}{s_1'} = \frac{1}{f_1}$$

These two equations can be solved simultaneously for the two unknowns, s_1 and f_1; the solutions are shown in Table 1.

s_1' =	92.9			
M	f_1	f_1 (in.)	s_1	s_1 (in.)
0.333333	69.7	2.7	278.7	11.0
0.25	74.3	2.9	371.6	14.6
0.2	77.4	3.0	464.5	18.3
0.166667	79.6	3.1	557.4	21.9
0.142857	81.3	3.2	650.3	25.6
0.125	82.6	3.3	743.2	29.3
0.111111	83.6	3.3	836.1	32.9
0.1	84.5	3.3	929.0	36.6

Table 1: Calculation of focal length, f_1, and image distance, s_1, for the calibration source. All units are in mm unless noted otherwise.

Our final lens selection for the calibration source is dictated by the available achromat lenses, and the reasonableness of the required s_1, which is excessive in some instances. An f=75 mm achromat lens is available, so our calibration optics will have these final characteristics:

D_1 = 25 mm

f_1 = 75 mm

s_1' = 92.9 mm (3.7 in.)

s_1 = 389.2 mm (15.3 in.)

M = 1/4.2

The 1-mm diameter calibration source will be projected into the test section to an image size of 238 μm (1 mm/4.2).

One final note regarding the use of an achromat lens for the calibration source. We need to project an *exact* image of the object (the blackbody) into the test section, as if the blackbody itself was placed inside, with all its colors focused to the same point. This eliminates the need to remove the test section each time we wish to calibrate the pyrometer. Simple lenses do not focus all colors of light to the same point because the refractive index of any material is a function of the wavelength of light. This is shown schematically in Figure 6. Achromat lenses are an attempt at correcting this problem, known as 'chromatic aberration', by cementing two elements of different refractive indexes together, which results in the total elimination of chromatic aberrations *at two wavelengths*, usually a blue and a red. Aberrations for the wavelengths between these are small, though not completely eliminated.

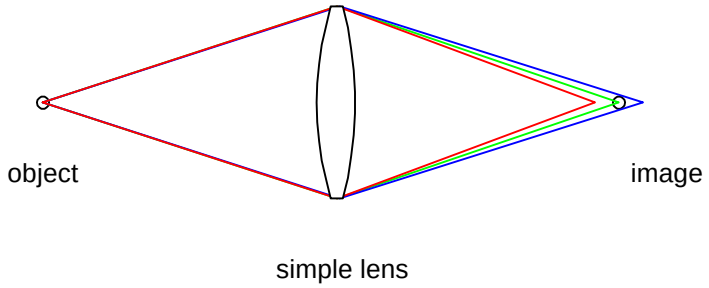

Figure 6: Schematic showing chromatic aberration caused by a simple lens.

The final component of the optical detection system is the high-speed camera. A conventional 35-mm SLR (single lens reflex) camera fitted with a 105-mm zoom lens is used. To achieve a higher magnification, a 25-mm extension tube is inserted between the lens and the camera body. The camera is operated in the manual mode with the shutter held open and all room lighting eliminated. The light emitted by the igniting and burning particles will thus be captured. To produce discrete images on the high-sensitivity black-and-white film, a chopper wheel is placed in front of the camera lens to provide 'shuttering' at approximate 500 Hz. Thus, one image will be recorded roughly every 2 ms of experiment time until the igniting particles leave the camera's field of view.

Goals for Next Quarter

During the next reporting period, we will continue to test and refine the pyrometer and the high-speed photography system. Thereafter we will begin to run experiments to measure ignition temperatures of the particles under various conditions, and to extract ignition rate constants. The high-speed photographs will show the ignition mechanism of the coals, and provide insight into the combustion behavior. The Distributed Activation Energy Model of Ignition will be modified to examine the effects of particle number and particle size distribution, as described earlier.